MECHANICAL LOADING TESTS ON IRRADIATED LWR FUEL RODS

D. PAPAIOANNOU, R. NASYROW, R. GRETTER, L. FONGARO, J. SOMERS, V. RONDINELLA
European Commission, Joint Research Centre, Directorate for Nuclear Safety and Security,
Karlsruhe, Germany
Email: Dimitrios.Papaioannou@ec.europa.eu

E. VLASSOPOULOS
Swiss Federal Institute of Technology in Lausanne (EPFL)
Lausanne, Switzerland

S. CARUSO
National Cooperative for the Disposal of Radioactive Waste (Nagra)
Wettingen, Switzerland

Abstract

During reactor operation, the mechanical properties of a nuclear fuel rod are radically altered. After discharge, alpha-decays and accumulated radiation damage or other processes associated to potential thermal variations occurring during interim storage, contribute to further ageing of the spent nuclear fuel (SNF). However, during all stages of the SNF management (handling, retrieval, packing and transportation to final disposal or reprocessing) safety must be guaranteed.

Assessment of the SNF mechanical stability against external stresses, which might be accidentally applied, requires representative reference data. Explicit tests simulating accidental conditions are conducted in the hot cells of JRC - Karlsruhe, in the frame of a multi task collaborative research programme. Three-point bending and gravitational impact devices were developed and installed in the hot cells to investigate the SNF rods response under quasi-static or dynamic loads. Load-deflection curves are generated in the 3-point bending tests, whereas a high-speed camera records the rod rupture during impact tests.

Results from investigations on LWR commercial fuel rods over an extended burn-up range are presented in this paper. SNF segments, pressurized at the original fuel rod pressure after discharge, were subjected to bending and impact tests. Similar masses, significantly less than a single fuel pellet, of fuel disperse upon pin rupture in both types of experiments. Only fuel fragments from the immediate vicinity of the rod fracture release. An image analysis methodology was developed to elaborate the sample's behaviour under dynamic loads. Optical and electron microscopy were used to observe the morphology, orientation and population of the cladding hydrides, whereas the overall hydrogen concentration in the cladding was measured with hot extraction technique. Size distribution analysis on the released fuel particles was also performed. The study is augmented by modelling approach to evaluate the individual phenomena and parameters affecting the SNF properties.

1. INTRODUCTION

In many countries producing nuclear energy, the interim storage of spent nuclear fuel (SNF) has been extended up to 100 years and beyond, until final geologic repositories will be constructed and commissioned [1]. At a certain point the temporarily stored fuel rods must be retrieved, handled, maybe repacked and transported to their ultimate disposal facilities. In this perspective, it is highly important in view of safety aspects to address the mechanical integrity of used fuel rods during and after storage, either under normal operational or even accidental conditions. In the case of a transport accident for instance, SNF rods might be fractured and fuel could come out of the cladding and disperse in the cask. The fuel release must not generate deleterious radiological consequences; even in the worst case of reconfiguration and accumulation inside the transport container, the criticality safety must be ensured.

The mechanical properties of nuclear fuel rods change massively during their operational life in the reactor. Irradiation of the fuel induces gas production, development of high burn-up structure (HBS) at the fuel periphery, cracking and swelling, gap closing and formation of pellet-cladding interaction (PCI) layer, which consequently enhance the hoop stress on the cladding. Presence of deleterious compounds in the PCI can also chemically affect the reliability of the cladding, whose ductility is anyhow strongly disturbed by irradiation and hydrogenation. Despite the lower dose rates and temperatures during storage than during irradiation, the fuel alterations do not end with discharge from the reactor. The continuous alpha-decays and helium build-up, in

particular after extended storage periods, results in further damage in the fuel and indirectly, in the cladding [2]. In addition, heating and cooling processes occurring during handling (discharge, followed by wet-dry interim storage) may affect the configuration of hydrogen in the cladding, causing hydride reorientation phenomena, which in turn affects its ductility and mechanical stability.

All these modifications may affect the response of spent fuel rods to external mechanical solicitations that might be applied during normal or accidental conditions. Several attempts, experimental and modelling approaches, have been conducted by the international research community to enrich the knowledge and the database underpinning such mechanisms. Many of these works are focussed on irradiated cladding properties by performing tests on defueled cladding ring specimens (ring compression tests). However, results from experiments on the composite fuel-cladding configuration, i.e. real SNF rods are extremely rare.

At the JRC - Karlsruhe, already in 2008, a simple free-falling hammer device inducing fuel rupture events was developed and installed in a hot cell. The impact tests were performed on irradiated commercial LWR UO_2 fuel segments with burn-ups between ~19 and ~74 GWd/tHM. The studies were carried out in the frame of collaboration and with the support of GNS (Germany) and AREVA NP and revealed important outcomes. Although the rigidly fixed SNF rod specimens ruptured over 3 breakages, totally 3.9 to 5.6 g coarse fuel fragments were released, i.e. 1.3g till 1.9 g per breakage. Details of those pilot tests can be found elsewhere [5].

In 2016, a new experimental campaign was started in JRC Karlsruhe to establish a basis of reference data and provide reliable conclusions by performing tests on SNF rod segments with own developed and dedicated equipment, designed specifically to be fit for purpose to meet these demands. The new campaign is partly based on collaborations with NAGRA (Switzerland) and BAM (Germany) [8–9] 00 and aims to determine the fuel rod response to external loads till failure. Segments with different properties (burn-up, fuel composition, history, cladding, etc.) are pressurized to the original rod pressure and subjected to quasi static — bending — or dynamic — impact — mechanical loading experiments. The critical fracture load (or better energy) and the fuel mass released are determined. Thorough characterisation of the fuel rod and concomitant specimens is carried out before and after each experiment for a comprehensive evaluation of the SNF rods behaviour. This paper presents an overview of the experimental approach, reports and comments on some representative results obtained so far and introduces preliminary principles towards a FE model development to utilize the experimental output.

2. EXPERIMENTAL SET-UP

The experiments are conducted at the hot-cell facilities of the JRC – Karlsruhe with two home developed devices, comprehensively described in Ref. [10] for 3-point bending and gravitational impact tests on fuelled, pressurised SNF rod segments. The force/energy required for a fuel rod to fail is determined under the experimental boundary conditions. As the accidental scenarios are limitless, it has been decided to study the SNF mechanical integrity under two reference conditions by applying quasi-static or dynamic loads. The acquired data are correlated to properties and processes that potentially affect the SNF mechanical stability. In addition to post irradiation examinations performed on the fuel rod at previous stages including many non- or destructive hot cell techniques, fuel and cladding of the tested specimen are extensively examined after the experiment too. Metallography at the direct vicinity of the failure location to investigate the hydride morphologies, population and orientation is implemented, whilst the local H_2 content is determined by means of the hot-gas extraction method. After dynamic impact the released fuel particles are observed by scanning electron microscopy (SEM) and corresponding size distributions are determined by image analysis.

The employed experimental set-ups are shown schematically in Fig. 1. The 3-point bending apparatus consists of a force transmitter fixed on loading column, which is driven perpendicular to the sample axis by a step-motor at a constant slow speed between 4 and 17 μm/s. The force transmitter, called “deflector” in this paper, has a concave round contact surface (see details in the insert schema in Fig. 1a), adjusted to the cladding shape, so that no other side or edge load is applied on the fuel rod segment during the experiment. The flexible modular design of the device allows the use of different loading transmitters or thanks to removable supports, different specimen lengths. The geometrical configuration of the device follows the prerequisites of a standard bending test as specified in the ISO 7438 standard [14]. The device is equipped with sensors for simultaneous acquisition of the applied load and the sample's deflection and internal pressure of the segment. The raw data are in the form of load-displacement curves. The loads are used to evaluate the stresses according to Eq. 1

$$\sigma_f = \frac{8FL}{\pi D^3} \tag{1}$$

where F, L and D are the mean values of the load, support span and rod diameter, respectively. The uncertainty associated to the reported flexural strength is derived based on the method described in Ref. [15].

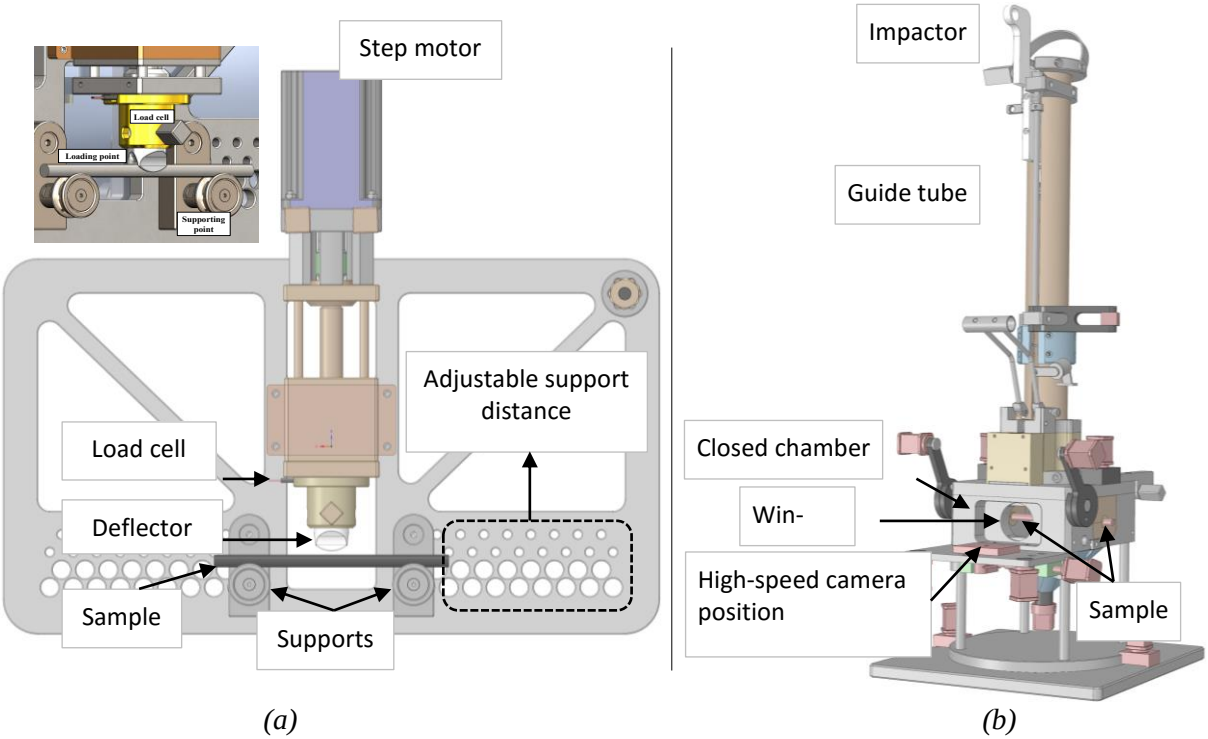

FIG. 1. Overview of the 3-point bending apparatus (a) and impact tower (b)

The new apparatus for impact tests, shown in Fig. 1b, is based on the same principles as the previous one used to perform the experiments reported in [5]. The specimen is impacted by a falling body (hammer), called "impactor" in this paper, through a vertical guiding column. However, the device has been significantly improved. In the new edition, the impact occurs in a closed chamber, where the released material (basically fuel, but also pieces of the outer cladding oxide layer) is completely captured. The coarse fragments are collected at the bottom thanks to the funnel shape of the chamber interior, whereas the fine aerosol particles settle on the internal walls, or are caught on the particulate filter of an integrated aspiration system. The impact of the specimen is video recorded by a high-speed digital camera (2000 frames/s) placed on the window of the chamber, provided with its own illumination.

As far as possible the design of the two devices is mutually consistent. In both experiments the specimens are bent or impacted by rounded compactors, as shown in Fig. 2. The main difference is related to the velocity of the impactor and bending deflector in the two experiments, enabling direct comparison of the results in both configurations. Indeed, the velocity of the falling hammer at point of impact is 3.5 m/s, i.e. at least $2x10^6$ times faster than in the 3-point bending test.

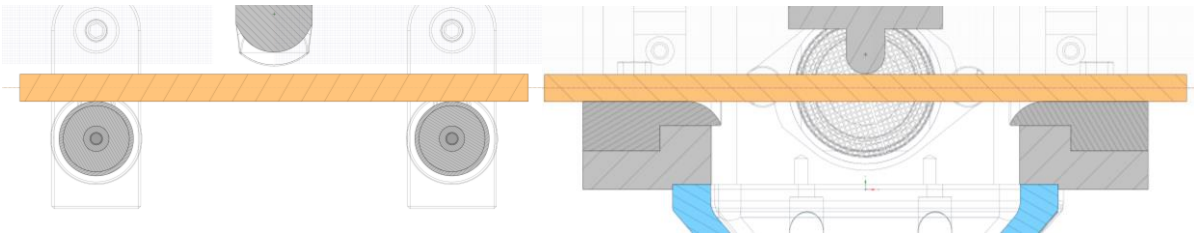

(a) *(b)*

FIG. 2. Scheme of the specimen positioning in the bending (a) and impact (b) device; rounded supports of same radius and specimen lengths are used for both experiments

The previous concept of the impact device has been significantly improved. In the installation used in Ref. [5] and for the experiment presented in Ref. [12], the specimens were rigidly fixed and were enforced to break at 3 positions upon impact. In the new version, the specimens simply rest on edge rounded supports (see Fig. 2b) without any fastening, i.e. replicating the shape of the roll supports of the bending machine (Fig. 2a).

A typical specimen for mechanical testing is presented in the photograph of Fig. 3. Using exact tube fittings to preserve the required tightness, 25–27 cm long segments cut from SNF rods are connected to a Helium gas flask, pressurised to the desired pressure and disconnected, after closing the attached gas valve. A pressure transducer, fixed on the other end of the segment provides continuous pressure control and instant detection of the rupture/crack, which is very important for the bending tests.

FIG. 3. Gas tight specimen assembly connected to pressure gauge and with attached pressure transducer, ready for mechanical testing

3. EXPERIMENTAL RESULTS

The Investigations in the hot cells include experiments on commercial SNF rods from light water reactors (LWR), pressurised to their corresponding internal pressure, as measured at the end of in-pile service. Bending and impact are conducted on sets on carefully selected rod segments, excluding segments close to the spacer grids of the fuel assembly, or if relevant, close to locations suspicious for cladding or fuel failures. Until now only UO_2 fuel rods were studied covering an extended burn-up (BU) range, from 18 to over 100 GWd/tHM. Studies on MOX SNF rods are also foreseen in the immediate future.

3.1. Tests on surrogates

Prior to their installation in a hot cell, the two devices presented above were extensively controlled for proper functionality and operation with tele-manipulators. Many cold trials with surrogate specimens carried out for this purpose. The simulant tests used hydrogenated Zry4 cladding tubes, filled with Al_2O_3 pellets and pressurised to 40 bar. Most of the obtained results from the bending tests were already reported Ref. [8] in the form displacement vs. hydrogen content (see Fig. 4). The present paper completes that data set and also provides the maximum loads required to rupture the cold specimens. Despite the enormous changes of the displacement

measured, the corresponding maximum loads persist in a very narrow range between 1.3 to 2.1 kN and seem, contrary to the displacement, little affected by the hydrogen concentration in the cladding.

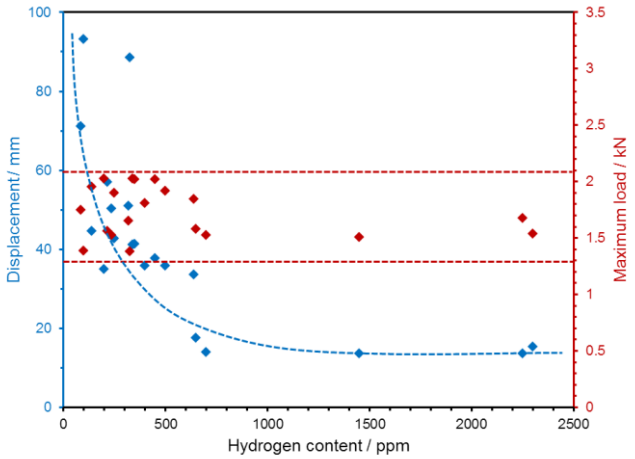

FIG. 4. Measured deflection and maximum load to fracture as a function of hydrogen concentration in the cladding during the cold 3-point bending test

3.2. Bending tests on SNF rod segments

Two load-displacement curves from the 3-point bending experiments on SNF rod segments with low and high average burn-up and corresponding hydrogen pick-ups, respectively, are compared in Fig. 5. The data were recently presented and extensively commented in Ref. [13]. A remarkable feature of this data is the instant drop of the applied load exactly at the point of the specimen fracture, i.e. at the very early stage of crack initiation. Roughly 20% higher loads were applied to rupture the high BU fuel segments, whereas its total displacement is less than half of the low BU rod. Considering the results from the cold test of Fig. 4, the overall behaviour of the SNF rods are in fair consistency. The higher displacement of the low BU specimen was expected, as the material preserves its ductility, but relatively small change in the maximum critical load to rupture was observed. Nearly 3 times more energy, as calculated by integrating the area under the curve, must be transmitted to the low BU fuel rod to induce its fracture. The different slopes of the curves in the elastic region denote the higher stiffness of the specimens. This is apparently caused by the higher hydrogenation of the cladding and closure of the gap between fuel and cladding.

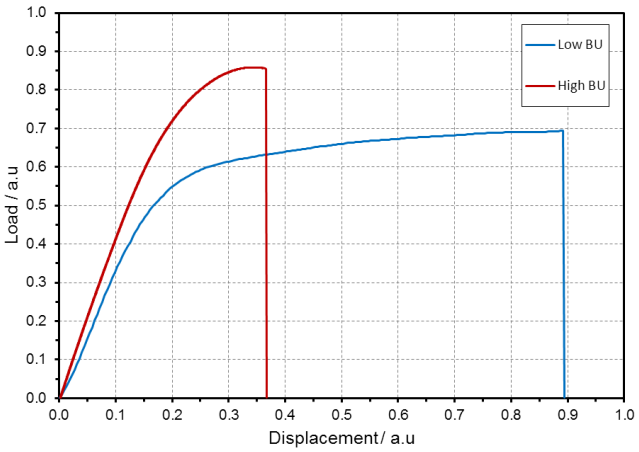

FIG. 5. Load-displacement curves of high and low BU samples during the 3-point bending tests

A segment from a PWR UO_2 fuel rod irradiated to a burn-up of ~67 GWd/tHM at the Grohnde nuclear power plant in Germany [16] has been subjected to a 3-point bending experiment. Table 1 summarises the main

features of the fuel rod tested. The metallography photograph of Fig. 6 shows the circumferentially oriented hydrides, many of them concentrated in the liner, in particular at the interface to the bulk material. Part of the outer oxide layer, as well as the closed gap and the formed pellet-cladding interaction layer are clearly visible. The segment was pressurised at 70 bar, as measured during puncturing and gas analysis carried out in the frame of the post irradiation examinations (PIE).

TABLE 1. MAIN FEATURES OF THE SNF ROD SUBJECTED TO MECHANICAL TESTING

Property	Characteristic/Value
cladding	duplex
pellet diameter	9.11 mm
outer diameter	10.75 mm
nominal cladding thickness	0.725 mm
peak outer oxide layer	~30 µm
hydrogen pick up	~300 ppm
Irradiation cycles	5
End of irradiation	March 2001
FGR (%)	13.6

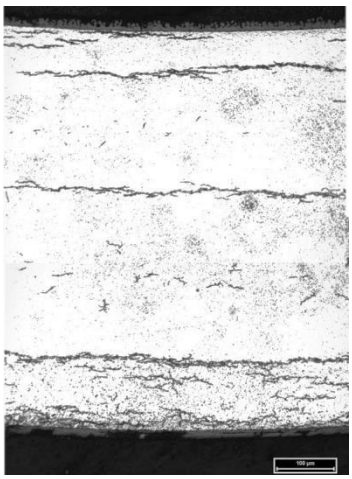

FIG. 6. Morphology and location of the hydrides in the duplex cladding of the 67 GWd/tHM SNF rod

During the 3 point bending test, performed with 4.9 µm/s translation of the deflector, the load, displacement and pressure were monitored online and are shown in Fig.7. The segment rupture was perfectly detected by both, load and internal pressure measurements. Fracturing caused an instant drop of the applied load and pressure in the specimen. However, the complete depressurisation took another 2 min, as the fuel is in strong contact with the cladding. The overall displacement from straight pin without contact of the deflector till rupture is 0.9 cm, whereas the maximum load reached 3 kN. The fuel mass released by weighing the specimen before and after experiment was 0.99 g, i.e. much less than the mass of a single fuel pellet.

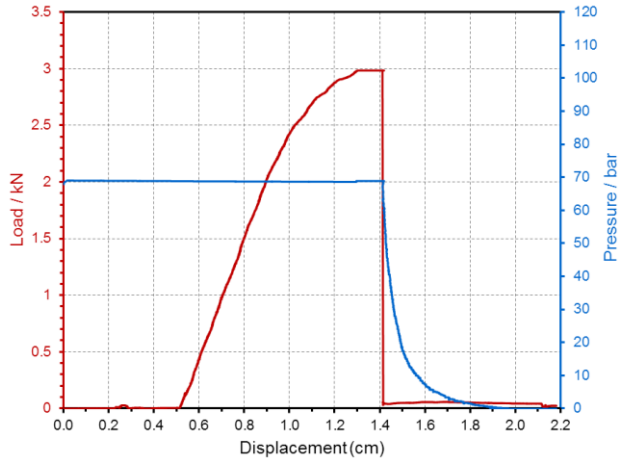

FIG. 7 Force and internal pressure development against displacement during the 3-point bending test of a 67 GWd/tHM SNF rod

It is interesting to compare this data with those on simulant specimens in Fig.4. Although the critical load for rupture is higher than the range found in the cold tests and the displacement till rupture around 3.5 times shorter, the agreement is still pretty fair, but one must highlight the failure of any simulant to entirely substitute the real irradiated composite fuel/cladding.

3.3. Impact tests on SNF rod segments

The impact device is not equipped with explicit sensors for the acquisition of load-displacement curves. Instead, a high-speed camera attached to the closed chamber of the apparatus records the tests. A sequence of images over a total collection time of only 6.1 ms obtained from the original video file are listed in Fig. 8. The visual inspection of the impact provides extremely valuable insight of various phenomena occurring. Image (a) shows the hammer just before touching the specimen. In the images (b) and (c) several splinters of the cladding's outer oxide layer are clearly propelled from the contact area between hammer and specimen. The crack initiation, morphology and propagation are revealed in image (c). The same photograph illustrates the moment of the “explosive” fuel release in form of a fine particle cloud. Finally, the subsequent progression and release of fuel coarse fragments at the opening of the crack is observed in images (d) and (e).

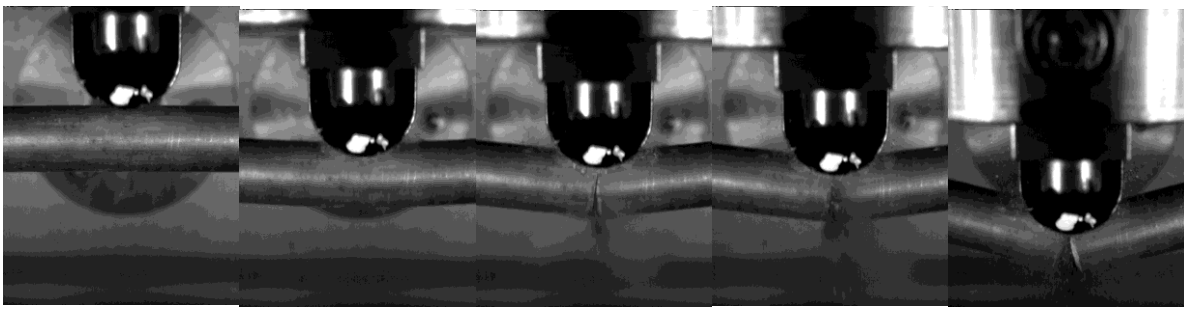

(a) *(b)* *(c)* *(d)* *(e)*

FIG. 8. Representative selected frames of the image sequence during an impact test on a SNF rod

Fig. 9 shows the image at the point of rupture for 3 different burn-up fuel segments. These results are in absolute conformity with the bending tests. Measured form the initial horizontal position, denoted by the red line in Fig. 9, the displacements at the moment of rupture decrease with increasing BU for SNF rods having the same cladding material. As with the bending results presented above, the deformation from the horizontal depends mostly on the hydrogen content in the cladding, which usually follows the burn-up.

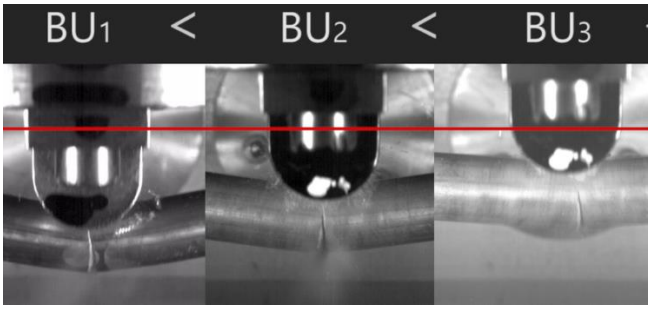

FIG. 9. High speed camera videos from different impact tests showing the aerosol release and total deflection from the initial horizontal position (red line) at the rupturing moments

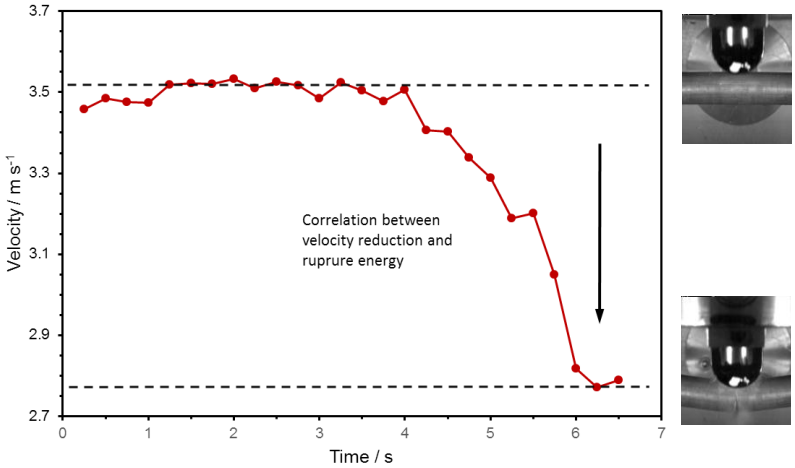

FIG. 10. The hammer velocity change is used to calculate the transmitted energy caused the specimen rupture

An image analysis (IA) methodology to extract velocity data from the video records is under development. The process converts the obtained impact sequence images into instantaneous sample deflection and hammer velocity. Thus, the kinetic energy transmitted by the hammer to the specimen can be calculated from the observed velocity reduction upon impacting, as illustrated in Fig. 10. The quantification of the uncertainty associated to the derived IA methodology has not been evaluated at this stage. A direct estimation of this uncertainty is very challenging, since it is depended on the minimum detectable displacement and applied object tracking algorithms, which can differ for each case.

The images presented in Fig. 8 were obtained from the video recorded for the impact test on the 67 GWd/tHM SNF rod, whose bending test results are presented in Fig.7. The impact test was performed by a 10.75 kg hammer. A total of 2.33 g of material was released upon fracturing, predominantly fuel, but also some fragments from the cladding oxide. The same fuel rod had also been tested with the previous configuration of the device. The specimen, fixed on the chamber walls, was impacted by an 8.5 kg hammer and broke in two parts via 3 breakages with an overall mass release of 2.44 g, i.e. 0.81 g per breakage. The majority of the released material was collected as coarse fragments, whereas ~0.05 g (2% of the total mass released) consisted of fine particulate deposited on the inner walls or collected on the aspiration system of the testing chamber. The results of this previous experiment were reported in Ref. [12].

After the second experiment presented here, the size distribution analysis was performed on the fuel particles deposited on the chamber inside walls. By swiping with adhesive conductive tapes, many of the released particles were collected and photographed on a scanning electron microscope (SEM). The fuel particles reveal a variety of morphologies, as they originate from different radial locations of the fuel pellet. The presence of relatively large (up to tens of microns in size) particles with the typical morphology of the high burn-up structure (HBS) confirms that recrystallised in high burn-up structure (HBS) areas do not necessarily fragment into individual grains, but rather following discrete cracking patterns. However, numerous sub-micron grains were also found. Cladding oxide particles were also detected but excluded from the analysis, as they were distinguished in the micrographs with the back-scattered (BS) technique. The micrographs were processed to classify the parti-

cles according to their equivalent circle diameter (ECD). Indicatively, two of the processed SEM micrographs and the resulting histogram are presented in Fig. 11. The histogram represents the average number of particles in each class found in all processed images. The red squares in the same plot are the average ECD in each class.

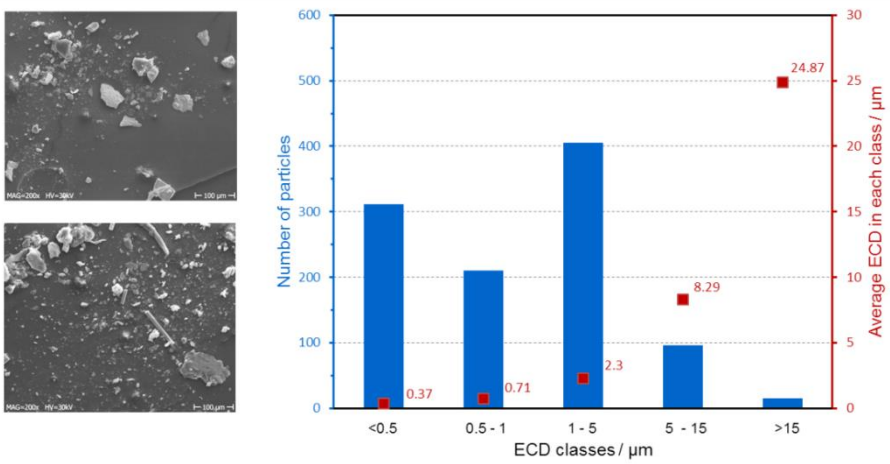

(a) *(b)*

FIG. 11. SEM micrographs (a) of particles released after bending and histogram (b) with their average population of each size class

4. NUMERICAL ANALYSIS OF THE TESTS

Numerical investigations via Finite Element Analysis (FEA) formed the second phase of the current study. This work complements the experimental activities Ref. [11] and contributes not only towards a better understanding of the SNF rod mechanical response under bending stresses, but also provides the means to assess conditions and configurations outside of the domain defined by the present experimental studies. The main objective of this campaign is the development and calibration of FE models against the experimental results to derive effective mechanical properties of the SNF rods. The final product of this study is the development of macroscale SNF, with its contaminant structural parts and fuel assembly models to investigate its mechanical integrity in various loading conditions (normal or accidental scenarios) for different back-end of the fuel cycle management actions (storage, transportation and handling).

A stepwise approach was followed to derive the effective mechanical properties of the composite fuel-cladding system. Therefore, the rod has been modelled initially as a simple beam element and integrating an explicit description of fuel and cladding. Since the experimental results describe macroscopically the mechanical behaviour of the rod, the simple beam element directly simulates the experimental results and the model can be calibrated against them. The mechanical propertied derived can only describe the specific type of fuel rod samples tests. To broaden the numerical results to different types of SNF rods, the tests were simulated and validated again by considering explicitly the cladding and the fuel pellets. A sensitivity analysis was performed to investigate the driving parameters and the relative influence of different phenomena to the rod's mechanical response, such as pellet-clad gap size, clad thickness, pellet positioning, etc.

The ANSYS mechanical tool is used for the development of the finite element models. Due to the difference in strain rate and boundary conditions (load application) between the 3-point bending and the impact test, two different models were created for the simulation of the two mechanical tests. For the displacement driven 3-point bending test, a step-motor is used to drive slowly the former onto the sample by applying quasi-static loads, whereas in the gravitational impact test dynamic loads are applied to the sample by the free-fall movement of the hammer. Therefore, 3D static structural models have been developed using the implicit and transient analysis (including inertia effects) for the bending and impact case, respectively. In the following paragraphs, the development of the cladding/pellet model for the bending case along with the applied sensitivity analysis is described.

4.1. Model description

The analogue studies with the use of the surrogate sample rods [8] are used as the basis for the development and calibration of the FEMs. The highly inhomogeneous material properties and geometrical configuration of the SNF prevents a direct investigation of individual phenomena (i.e. pellet-cladding mechanical interaction (PCMI), Zr hydride orientation and/or concentration, etc.). In contrary, the "cold-test" campaign is conducted with well-known materials, thus a number of geometrical and material introduced uncertainties are excluded. This facilitates a deeper understanding of the physics and phenomena involved during the tests governing the mechanical response of the rodlets.

The model involves large deformation effects and it is highly non-linear. As seen from the 3-point bending test results, even the SNF rods with high burn-up experience plastic deformation. In this situation, the analysis evolves form linear (elastic behaviour) to non-linear (elasto-plastic behaviour). Therefore, the selection of various model parameters might introduce numerical uncertainties that could potentially influence the results. For the derivation of a final model, a sensitivity analysis was performed to investigate the relative importance of different parameters, such as the contact method, the element type and mesh quality, the friction coefficient, the material laws, the boundary conditions and many others. The numerical results are compared against the experiment and focus was given on specific outcomes, such as the CPU time, max stresses at cladding and pellets and maximum contact pressure and penetration. The final model is derived as the best compromise between the simulation time and the numerical accuracy.

As a result, the pellets are modelled as cylindrical solid elements with flexible behaviour [9]. Since ceramic materials have significant difference in tension and compression, the ANSYS "cast-iron" plasticity model has been used to describe their behaviour. The model assumes isotropic elastic behaviour, but different plastic yielding and hardening in tension and compression. A compression to tension ratio parameter was used to account for this effect. The cladding has been modelled both as a shell and a body element. Though the surface element was advantageous in terms of computational time, enhanced numerical convergence was achieved with the use of the body element. Therefore the latter approach was chosen. The "Voce" hardening law was used to model the non-linear isotropic hardening. The former and the supports are modelled as shell elements with rigid behaviour. To reduce the number of elements and minimize the computational time, 1/4 symmetry was introduced. Quasi-static loads were applied by assigning a maximum deflection to the former in accordance to the experimental results.

The model was calibrated against the experimental results with the use of the optiSLang tool, an ANSYS integrated software package for sensitivity analysis and optimisation. In brief, certain variables of the model are parametrised (which in this case are the material properties), so their relative importance at the final results can be explored by optiSLang [13, 17]. An objective function is created by comparing the load-displacement curve as derived from the simulation to the experimental results. optiSLang explores the solution space of this optimisation problem by intelligently generating a number of FEA simulations by varying the parameter values. As initial values and variable range for the model parameters linked to fuel and cladding, experimental data (e.g. elastic modulus) found in the open literature are used. The driving parameters of the model are further adjusted till finally the model calibration is achieved by minimizing the difference between predicted and experimental results. Fig. 12 shows the load-displacement curve comparison for the generated FEA simulation against the experimental results. The "best-fit" has been highlighted in red showing an almost perfect match to the experimental derived curve (black).

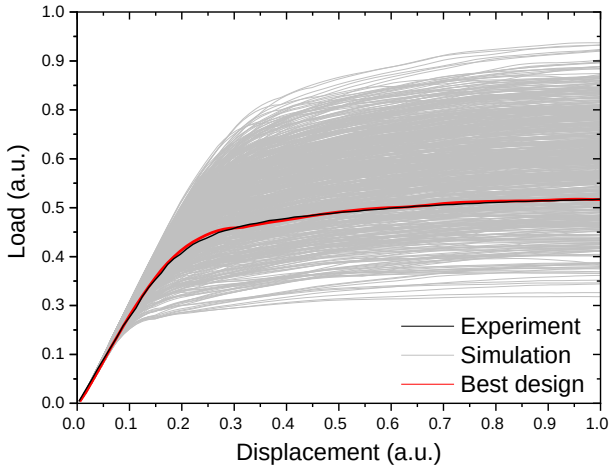

FIG. 12. A series of simulations (grey) with the experimental data (black) and best fit (red)

Fig. 13 provides the pellet-cladding equivalent (von-Misses) stresses for a deflection of 15mm (right) at the symmetry z-plane, where a snapshot of the rod's bending is given on the left part. It is noticed that the maximum stresses are developed at the inner cladding surface subjected to tension (opposite to the deflector) and the pellet-pellet interphase closest to the applied load (symmetry z-plane). This explains the importance of the pellets position in conjunction to crack initiation and demonstrates the weakest points that might endanger the cladding integrity.

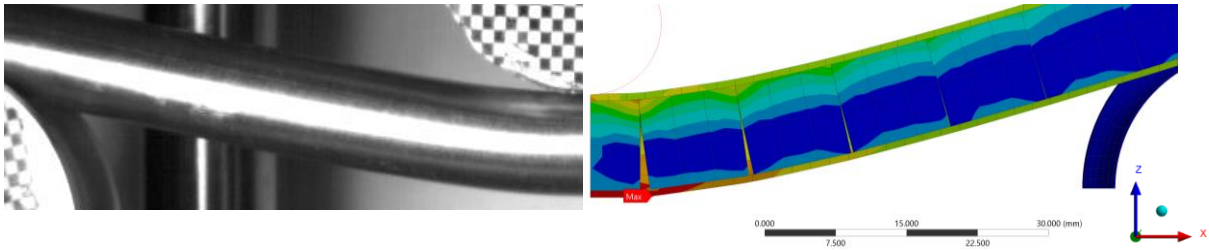

FIG. 13. Equivalent (von-Mises) stresses at a rod displacement of 1.5 mm at the symmetry z-plane. Maximum stress indication at the inner clad surface subjected in tension and at the closest pellet-pellet interphase to the theoretical maximum applied load (symmetry plane).

5. SUMMARY AND CONCLUSIONS

Experimental and numerical studies are performed at JRC Karlsruhe and NAGRA, respectively to assess the mechanical integrity of SNF rods against external solicitations that might occur during accidental conditions. Exclusive devices were developed and commissioned for 3-point bending and impact tests at the hot cells. Experiments were initially performed on surrogate specimens, but then once the equipment had been proven, on irradiated fuel rod segments. The tests performed cover a wide range of burn-ups and other aspects relevant to mechanical stability and safety issues during handing and transportation of SNF rods, especially after extended storage periods. The experimental conditions selected were focussed on quasi-static or dynamic impact of pressurised (to the rod's original internal pressure) specimens, considering them as two reference situations for a potentially infinite set of accidental scenarios.

The load-displacement curves acquired from the 3-point bending tests demonstrate the correlation between preserved ductility with burn-up. All specimens studied experience plastic deformation before cracking, but the low BU segments preserve ductility at higher deformations than the high BU SNF rods. Higher stiffness resulting low deformation till rupturing and strength were measured for high BU fuel rods. In opposite, low burn-up fuel rods achieve larger displacements and require roughly 20% lower forces till they crack.

The mechanical response of the SNF rods under impact was evaluated with dedicated image analysis of videos recorded by a high-speed camera. The analysis provides essential information on failure mode, crack

initiation and propagation and detailed data including the instantaneous impactor's velocity, applied loads and transmitted energy to the specimen, enabling correlation between mechanical properties of the cladding/fuel system in different strain rates. The released fuel upon fracturing in form fuel aerosol-fine, coarse particles or fragments are collected and subjected to size analysis.

In all conducted bending and impact experiments the overall released masses never exceeded the mass of a single fuel pellet. The majority is dispersed in form of fragments, which in the case of the impact tests are collected at the bottom of the device chamber. Only a small fraction of the fuel released is dispersed as fine particles, which, as seen in the recorded high-speed camera videos, are floating in the testing chamber till they finally deposit on the chamber walls or captured by the filters of the aspiration system.

The results of the bending and impact experiments of a PWR 67 GWd/tHM UO_2 were presented. After an overall displacement of 9 mm and maximum force 3 kN the pressurised at 70 bar specimen ruptured and 0.99 g material released. Detail characterisation of the released material carried out after the impact test. The majority, around 98% of the totally 2.33 g released mass were found at the bottom of the testing chamber. The fine fuel particles collected were originating from different pellet regions and the image analysis of the SEM micrographs revealed their size distribution, ranging from sub-micron to greater than 15 µm. The difference in the released masses between the bending and impact experiment lies in the different loading and rupturing approaches (static vs. dynamic). It might be also due to the pellets positions in the loaded areas. However, they are in both tests of the same order of magnitude.

There is still a need for more tests (e.g. dependence on fuel composition, irradiation and post-irradiation history, type of cladding and hydrides content). Mechanical tests on MOX SNF rods are of highest priority in the programme. Isolating cladding hydrides effects in the overall mechanical behaviour of irradiated fuel rods is also foreseen.

The experimental tests have been simulated by static and transient structural Finite Element (FE) models based in the ANSYS mechanical software platform. The first approach assumes certain simplifications related to the pellet-pellet and pellet-cladding interactions. Once the models are calibrated and verified, the derivation of sophisticated rod failure criteria is examined as a function of material property evolution with burn-up. The numerical analysis in the final state intents the development of macro-scale models (SNF assemblies and structural parts) to study the mechanical integrity in various scenarios (transportation, handling, etc.).

ACKNOWLEDGEMENTS

The present scientific-technical results support the Member States in implementing the Council Directive 2011/70/EURATOM on responsible and safe management of spent fuel and radioactive waste. It is directly coupled to the Article 12.1(f) stating the need to perform "the research, development and demonstration activities that are needed in order to implement solutions for the management of spent fuel and radioactive waste".

Deeply appreciated are the contributions to this work of Mr. Gianni Paperini and Mr. Frederic Laheurte, both members of the hot cells team at JRC – Karlsruhe, who performed the microscopy examinations. The authors are thankful to the Gösgen nuclear power plant (KKG) and Framatome GmbH (former AREVA GmbH) for their support providing and authorising the employment of some SNF rods for the mechanical studies. We are especially indebted to Dr. Fabian Jatuff, Mr. René Sarrafian and Dr. Bruno Zimmermann from KKG, who greatly supported the realisation of this project. Finally, we thank Dr. Wolfgang Goll, Dr. Elmar Werner Schweitzer and Dr. Klaus Nissen from Framatome GmbH for their useful insights and comments.

REFERENCES

[1] Extended Storage Collaboration Program International Subcommittee Report, Report 1026481, EPRI (2012).

[2] RONDINELLA, V.V., et al., Proc. PSAM11-ESREL 2012, June 25-29, 2012, Helsinki, Finland.

[3] RONDINELLA, V.V., et al., Proc. IHLRWMC 2015, Charleston, Apr 12–16, ANS, p. 12715 (2015) 479-485.

[4] WISS, T., et al., J. Nucl. Mater., **451** (2014) 198-206.

[5] PAPAIOANNOU, D., NASYROW, R., RONDINELLA, V.V., GOLL, W., WINKLER, H.-P., LIEDTKE, R., HOFFMANN, D., Proc. KTG 2009, May 12-14, 2009, Dresden, Germany.

[6] INTERNATIONAL ATOMIC ENERGY AGENCY, Final Report CRP SPAR III, IAEA-Tecdoc-1771, IAEA, Vienna (2015).

[7] RONDINELLA, V.V., WISS, T., PAPAIOANNOU, D., NASYROW, R., CAPPIA, F., VAN WINCKEL, S., SERRANO-PURROY, D., WEGEN, D., Proc. IHLRWMC 2015, Charleston, April 12 – 16, Paper 12715 (2015) 479-485.

[8] NASYROW, R., PAPAIOANNOU, D., RONDINELLA, V.V., VLASSOPOULOS, E., LINNEMANN, K., BALLHEIMER, V., STERTHAUS, J., ROLLE, A., WILLE, F., CARUSO, S., Proc. 18th Int. Symp. Packaging and Transportation of Radioactive Materials (PATRAM 2016), paper 6023, Sept. 18-23, 2016, Kobe, Japan.

[9] LINNEMANN, K., BALLHEIMER, V., STERTHAUS, J., ROLLE, A., WILLE, F., NASYROW, R., PAPAIOANNOU, D., VLASSOPOULOS, E., RONDINELLA, V.V., Proc. 18th Int. Symp. Packaging and Transportation of Radioactive Materials (PATRAM 2016), paper 2012, Sept. 18-23, 2016, Kobe, Japan.

[10] VLASSOPOULOS, E., CARUSO, S., NASYROW, R., PAPAIOANNOU, D., GRETTER, R., RONDINELLA, V.V., Nagra Working Rep. NAB 16-067: Investigation of the properties and behaviour of spent nuclear fuel under conditions relevant for interim dry storage, handling and transportation: experimental setup optimisation and cold test campaign, Wettingen, (2017).

[11] VLASSOPOULOS, E., NASYROW, R., PAPAIOANNOU, D., RONDINELLA, V.V., CARUSO, S., PAUTZ, A., Proc. IHLRWMC 2017, Charlotte, April 9 – 13, Paper 19902 (2017) 726-733.

[12] RONDINELLA, V.V., NASYROW, R., PAPAIOANNOU, D., VLASSOPOULOS, E., CAPPIA, F., DIESTE-BLANCO, O., WISS, T.A.G., "Mechanical integrity studies on spent nuclear fuel rods", Proc. IHLRWMC 2017, Charlotte, April 9-13, Paper 19921 (2017) 734-740.

[13] VLASSOPOULOS, E., NASYROW, R., PAPAIOANNOU, D., GRETTER, R., FONGARO, L., SOMERS, J., RONDINELLA, V. V., CARUSO, S., GRÜNBERG, P., HELFENSTEIN, J., SCHWIZER, P., PAUTZ, A., Response of irradiated nuclear fuel rods to quasi-static and dynamic loads, KERNTECHNIK **83** (2018) 6.

[14] ISO 7438:2016, Metallic materials - Bend test

[15] ŠTUBŇA, I., ŠÍN, P., TRNÍK, A., VOZÁR, L., Measuring the Flexural Strength of Ceramics at Elevated Temperatures – An Uncertainty Analysis, Measurement Science Review **14** 1 (2014)

[16] ARBORELIUS, J., DAHLBÄCK, M., HALLSTADIUS, L., JOURDAIN, P., ANDERSSON, T., LISDAT, R., HAHN, M., TOSCANO, E.H., Zirconium in the Nuclear Industry: 14th Int. Symp., ASTM International, West Conshohocken, PA (2004).

[17] VLASSOPOULOS, E., PAPAIOANNOU, D., NASYROW, R., CARUSO, S., RAFFUZZI, V., GRETTER, R., FONGARO, L., SOMERS, J., RONDINELLA, V.V., GRÜNBERG, P., PAUTZ, A., HELFENSTEIN, J., SCHWIZER, P., Mechanical Integrity of Spent Nuclear Fuel: From Experimental to Numerical Studies, TOPFUEL 2018, ENS, Prague (2018).